Chiral Tailor-Made Solvents and Their Impact on Solution Thermodynamics and Crystallisation Kinetics of Mandelic Acid

4 authors, including:

Dr.-Ing Samuel Kofi Tulashie
University of Cape Coast
40 PUBLICATIONS **258** CITATIONS

SEE PROFILE

Jan Von Langermann
University of Rostock
81 PUBLICATIONS **894** CITATIONS

SEE PROFILE

Heike Lorenz
Max Planck Institute for Dynamics of Complex Technical Systems
222 PUBLICATIONS **2,029** CITATIONS

SEE PROFILE

DOI: 10.1021/cg101179y

CRYSTAL GROWTH & DESIGN Article

2011, Vol. 11
240–246

Chiral Task-Specific Solvents for Mandelic Acid and Their Impact on Solution Thermodynamics and Crystallization Kinetics

Samuel K. Tulashie,[†] Jan von Langermann,[†] Heike Lorenz,*[,†] and Andreas Seidel-Morgenstern[†,‡]

[†]*Max Planck Institute for Dynamics of Complex Technical Systems, Sandtorstrasse 1, 39106 Magdeburg, Germany, and* [‡]*Otto von Guericke University, Chemical Process Engineering, Universitätsplatz 2, 39106 Magdeburg, Germany*

Received September 6, 2010

ABSTRACT: The synthesis and application of enantiopure short-chain mandelic acid esters as chiral task-specific solvents were investigated for the determination of hetereochiral interactions between chiral solutes and chiral solvents. Because of specific chiral interactions between the mandelic acid enantiomers as solutes and the *S*-configured solvents for this chiral system, asymmetric behavior was elucidated. Differences for (*R*)- and (*S*)-mandelic acid were determined with respect to solution thermodynamics and crystallization kinetics for the chiral solvents (*S*)-mandelic acid *n*-propyl ester [(*S*)-*n*-propyl mandelate] and (*S*)-mandelic acid isopropyl ester [(*S*)-isopropyl mandelate]. These differences were explained via evaluation of enantiospecific interactions applying molecular modeling methods.

1. Introduction

Within the pharmaceutical industry, the chemical synthesis of chiral substances provides usually only racemates with 50:50 mixtures of the enantiomers.[1] On the other hand, most of the chiral drugs are produced in the form of single enantiomers; often only one of the enantiomers shows the desired properties. Hence, enantioseparation is an important task in pharmaceutical development.[2] Moreover, on the basis of the benefits of single enantiomers and the size of the chiral market, production of enantiopure substances via separation processes such as crystallization has become very profitable.[3] Additionally, the resolution of enantiomers is directly related to the specific properties of the substance. Chiral systems are divided into (a) racemic compound-forming systems (90−95% of all cases), (b) conglomerates (5−10%), and so-called (c) pseudoracemates (rare) (Figure 1).[3]

These classes of substance possess different properties, which need to be considered within crystallization processes. Related to the final separation process is the important choice of an adequate solvent for the crystallization process, which directly influences the final yield, the crystal morphology, the appearance of solvates or polymorphic varieties, and the purity of the product.[4,5] Furthermore, the metastable zone width (MSZW) is also related to the choice of the solvent and therefore a very important key parameter for crystallization processes.[6] In classical achiral solvents, no differences are found between the two enantiomers.

However, for chiral solvents, these substances are expected to be able to create selective interactions with a chiral solute, which facilitates a differentiation between the two single enantiomers.[7,8] This discrimination can provide selective kinetic or solution thermodynamic effects, which might be useful for the separation of enantiomers. These dynamic interactions between solvent molecules and the related solutes are the background for almost any process within the solution, including solubilization.[9] Typical relations are ion−dipole, dipole−dipole, dipole−induced dipole, instantaneous dipole−induced dipole, hydrogen bond,[10] electron pair donor−electron pair acceptor, and solvophobic interactions.[11] Because of their unique physical and chemical properties, these interactions lead to specific properties and therefore also different macroscopic effects, e.g., differences in solubility, activity coefficients, etc. This includes the mentioned interactions between the solvent molecules and the solute as well as other solvent molecules or solutes, e.g., additives or liquid crystals.[12,13] Additionally, sterical effects from the molecules, irrespective of their chemical composition and structures, also might induce secondary interdependencies, for example, variations to a less stable conformation.[14] This influence on chemical structures becomes particularly important in the case of chiral systems, which includes the differentiation by formation of diastereomeric adducts.[15] From this effect, an asymmetry in the corresponding enantiomeric system and therefore an advantage in the resolution of chiral substances could exist. A literature search has shown a lack of systematic and clear experimental work with regard to the application of chiral solvents for enantioseparation. Mainly differences in thermodynamics were found, e.g., solubility. Yamamoto et al. reported pure enantiomer solubilities for a chiral cobalt salt in (2*R*,3*R*)-(+)-diethyl tartrate and described measurable differences between them.[16] Amaya provided a theoretical framework to account for the differences in solubility between D- and L-optical isomers in a chiral solvent, however without any experimental evidence.[17] Further, Bosnich and Watts[18] and Mizumachi[19] reported that the solubilities of the pair of enantiomers of *cis*-$[Co(en)_2Cl_2]ClO_4$ in (−)-2,3-butanediol and tri-α-diimine ruthenium(II) complexes, respectively, were different. Recently, Tulashie et al. observed that mandelic acid in (*S*)-ethyl lactate and (2*R*,3*R*)-diethyl tartrate showed a behavior comparable with that of normal achiral solvents.[20] In contrast to these thermodynamic effects, deviations were found in kinetic effects, e.g., metastable zone width.[21] For

*To whom correspondence should be addressed: Max Planck Institute for Dynamics of Complex Technical Systems, Sandtorstrasse 1, 39106 Magdeburg, Germany. Phone: (0049) 391 6110 293. Fax: (0049) 391 6110 524. E-mail: lorenz@mpi-magdeburg.mpg.de.

 Published on Web 11/17/2010

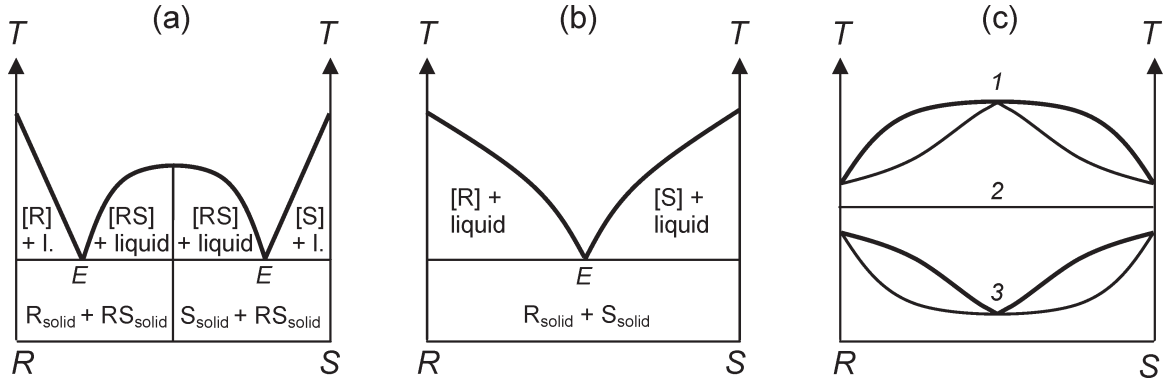

Figure 1. Melting point phase diagrams of crystalline chiral substances: (a) racemic compound, (b) conglomerate, and (c) pseudoracemate (continuous row of mixed crystals) (1, with maximum; 2, ideal; and 3, with minimum); E, eutectic; l., liquid.

example, because of the different rates of nucleation, D-isopropyl tartrate and (−)-(*R*)-pinene were successfully separated via chiral solvents.[22] For crystallization-related investigations, the influence of additives with similar structural identities was also discussed, e.g., L- or D-lysine for the separation of DL-glutamic acid and L-cysteine for DL-asparagine.[23,24] The usage of task-specific substances was also shown to influence nucleation, growth, and dissolution.[13,25,26]

In comparison, distinct similarities in the structure between the solvent and solute seem to be helpful for the creation of the desired effect. In this work, the usage of chiral task-specific solvents for the resolution of the compound-forming system mandelic acid was investigated. Particular attention was paid to the choice of a suitable chiral task-specific solvent. Because structural similarities could enhance the chances of asymmetric behavior, several esters of (*S*)-mandelic acid were synthesized, characterized, and tested.

2. Experimental Section

2.1. Materials. Racemic mandelic acid, (*S*)-(+)-mandelic acid, (*R*)-(−)-mandelic acid, concentrated sulfuric acid, ethanol, and sodium chloride were purchased from Merck; *n*-propanol, diethyl ether, (*S*)-(+)-methyl mandelate, potassium carbonate, and sodium sulfate were from Sigma-Aldrich, and 2-propanol was from VWR. The NMR solvent $CDCl_3$ was obtained from Deutero. Deionized water was used throughout the studies. All substances were used without any further purification.

2.2. Synthesis of the Chiral Task-Specific Solvents. The synthesis of the mandelic acid esters (mandelates) was adopted from Basavaiah et al.[27] and slighty modified (Scheme 1). (*S*)-Mandelic acid (50 g, 0.329 mol) was dissolved in an excess of the corresponding alcohol (see Table 1); 25 drops of concentrated sulfuric acid was added, and the mixture was refluxed for 3−4 h. Afterward, the remaining alcohol was removed under reduced pressure. The resulting crude ester was taken into 275 mL of diethyl ether, washed with aqueous K_2CO_3, followed by saturated aqueous NaCl, and finally dried over Na_2SO_4. After removal of the diethyl ether, the crude ester was distilled under high vacuum for purification. The yield of the esters was 60−65%. The purity, determined via DSC and NMR (^{1}H NMR and ^{13}C NMR), was ≥99%. The chiral task-specific solvents were freshly prepared before further usage.

2.3. Solvent Characterization. The determination of the melting temperatures and enthalpies of the mandelic acid esters synthesized was executed with the DSC131 differential scanning calorimeter from Setaram. An external chiller was used to facilitate the measurements of the low melting temperatures of the mandelic acid esters. Heating scans were performed at a rate of 1 K/min with helium as the purge gas. A sample contained 10−17 mg of the corresponding mandelic acid derivatives. An exemplary result is given in Figure 2 for (*S*)-isopropyl mandelate.

Table 1. Amounts of Solvent for the Synthesis of Mandelates[a]

alkyl residue	alcohol	volume (mL)
ethyl (Et)	ethanol	475
n-propyl (*n*-Pr)	*n*-propanol	625
isopropyl (*i*-Pr)	2-propanol	625
n-butyl (*n*-Bu)[b]	*n*-butanol	750

[a] NMR data. (*S*)-Mandelic acid methyl ester [(*S*)-methyl mandelate]: ^{1}H NMR (400 MHz, $CDCl_3$) δ 2.9−3.65 (s, 1H), 3.76 (s, 3H), 5.18 (s, 1H), 7.26−7.41 (m, 5H); ^{13}C NMR (100 MHz, $CDCl_3$) δ 174.1, 138.2, 128.6, 128.5, 126.6, 72.9, 53.1. (*S*)-Mandelic acid ethyl ester [(*S*)-ethyl mandelate]: ^{1}H NMR (400 MHz, $CDCl_3$) δ 1.15−1.24 (m, 3H), 3.9−4.3 (m, 3H), 5.16 (t, 3H), 7.23−7.36 (m, 5H); ^{13}C NMR (100 MHz, $CDCl_3$) δ 173.4, 138.3, 128.3, 128.1, 126.3, 72.7, 61.8, 13.7. (*S*)-Mandelic acid *n*-propyl ester [(*S*)-*n*-propyl mandelate]: ^{1}H NMR (400 MHz, $CDCl_3$) δ 0.8 (t, 3H), 1.59 (p, 2H), 4.11 (m, 2H), 5.17 (s, 1H), 7.25−7.51 (m, 5H); ^{13}C NMR (100 MHz, $CDCl_3$) δ 173.6, 138.4, 128.4, 128.2, 126.4, 72.8, 67.5, 21.7, 10.0. (*S*)-Mandelic acid isopropyl ester [(*S*)-isopropyl mandelate]: ^{1}H NMR (400 MHz, $CDCl_3$) δ 1.13 (d, 3H), 1.30 (d, 3H), 5.06−5.12 (p, 1H), 5.14 (s, 1H), 7.33−7.44 (m, 5H); ^{13}C NMR (100 MHz, $CDCl_3$) δ 173.2, 138.6, 128.5, 128.3, 126.4, 72.9, 70.2, 21.7, 21.4. (*S*)-Mandelic acid *n*-butyl ester [(*S*)-*n*-butyl mandelate]: ^{1}H NMR (400 MHz, $CDCl_3$) δ 0.84−0.88 (t, 3H), 1.2−1.28 (q, 2H), 1.51−58 (m, 2H), 4.09−4.2 (m, 2H), 5.17 (s, 1H), 7.28−7.48 (m, 5H); ^{13}C NMR (100 MHz, $CDCl_3$) δ 173.7, 138.4, 128.4, 128.2, 126.4, 72.8, 65.8, 30.3, 18.7, 13.4. [b] Because of problems with regard to the removal of small impurities, this solvent was not used for further investigations.

Scheme 1. Synthesis of Mandelic Acid Ester (mandelate)

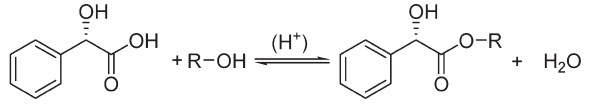

A Perkin-Elmer polarimeter (model 341) was used for the determination of the optical rotation angles at 20 °C with 10 cm cuvettes at a wavelength of 589 nm. The measurements were taken at 20 °C for (*S*)-ethyl mandelate and (*S*)-*n*-propyl mandelate and at 50 °C for (*S*)-isopropyl mandelate, because of its high melting point. ^{1}H (400 MHz) and ^{13}C (100 MHz) NMR spectra were recorded in $CDCl_3$ solutions on a Bruker DPX 400 spectrometer at 25 °C. Chemical shifts were referenced to TMS. Boiling points were determined with a B-540 melting point instrument from Büchi with a heating rate of 5 K/min between 150 and 300 °C.

2.4. Solubility Measurements. 2.4.1. Isothermal Method [mandelic acid in (*S*)-isopropyl mandelate]. Solubility measurements for mandelic acid in (*S*)-isopropyl mandelate were performed at 50 °C by applying a classical isothermal method. A known composition of mandelic acid enantiomers in (*S*)-isopropyl mandelate was prepared (leaving an excess of the solid phase), placed into a thermostated apparatus, and magnetically stirred at a constant

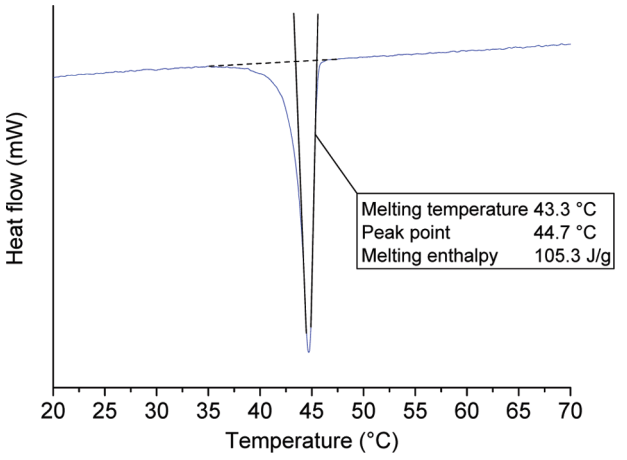

Figure 2. Differential scanning calorimetry result for (*S*)-isopropyl mandelate.

temperature (within ±0.01 K) until equilibrium was reached. Subsequently, the liquid and solid phases were separated and analyzed. The saturated solution was filtered for analysis with a glass filter (pore size of 10 μm). Samples of 1−3 mL were withdrawn from the filtrate for an evaluation of concentration. Hereby, the concentrations were determined by means of a refractometer (Mettler-Toledo). This was done by correlating the measured refractive indices with a calibration curve to evaluate the concentrations. Solubility values were obtained for (*S*)-mandelic acid, (*R*)-mandelic acid, and racemic mandelic acid.

2.4.2. Polythermal Method [mandelic acid in (*S*)-*n*-propyl mandelate]. Because only small quantities of the chiral solvent, (*S*)-*n*-propyl mandelate, were available for the experiments, the Crystal16 equipment from Avantium Research and Technology was employed for the solubility measurements. Crystal16 is a multiple-reactor system that can hold 16 (4 × 4) standard HPLC glass vials (11.5 mm diameter, flat bottomed, 1.8 mL volume). Herein, a polythermal method was applied by charging the reactor blocks with a supersaturated solution with known concentrations of (*R*)- and (*S*)-mandelic acid in (*S*)-*n*-propyl mandelate. The setup was heated until the solids introduced into the solvent were completely dissolved (heating rate of 0.5 K/min) and then cooled to recrystallize all samples at −10 °C (cooling rate of −0.5 K/min). With a heating rate of 0.04 K/min, the final solubilities were determined via turbidity sensors. Afterward, the evaluated saturation temperatures were plotted as a function of the corresponding concentration generating the final solubility curve.

2.5. Metastable Zone Width (MSZW) Measurements. Data of the so-called metastable zone width (MSZW) with regard to primary nucleation were determined for (*R*)- and (*S*)-mandelic acid in (*S*)-*n*-propyl mandelate. The experiments and the analysis were conducted using the polythermal method as described by Nyvlt et al.[28] Saturated solutions of ∼20 g were used. The solutions were subjected to a heating and cooling program related to the saturation temperature (T_{sat}) of the system. The initial concentrations were adjusted on the basis of the results of the solubility data. Solutions were prepared and placed into a batch crystallizer with a volume of 60 mL. Nucleation and dissolution were observed by means of an inline-turbidity sensor (QR-System, BASF AG, Ludwigshafen, Germany) and a Pt-100 temperature sensor. The MSZW for primary nucleation can be expressed as the maximum possible subcooling (ΔT_{max}), according to eq 1.

$$\Delta T_{max} = T_{sat} - T_{nucleation} \quad (1)$$

where T_{sat} is the saturation temperature (K) and $T_{nucleation}$ the nucleation temperature (K).

The quantity of ΔT_{max} was measured at different cooling rates. Finally, the values were extrapolated to a theoretical cooling rate of zero to obtain $T_{nucleation}$ for a given solution composition. The obtained ΔT_{max} data are valid for the experimental setup used and depend on, for example, the reactor size and geometry, the stirrer type, and the speed. In the case of the other chiral task-specific solvent, (*S*)-isopropyl mandelate, solutions were very viscous, and therefore, a determination of $T_{nucleation}$ could not be realized.

2.6. Solid Phase Analysis. The solid phases of all samples were studied by X-ray powder diffraction (XRPD), using a PANalytical X'Pert Pro diffractometer (PANalytical GmbH) with Cu Kα radiation. The samples were measured on Si background-free sample holders and scanned between diffraction angle of 3° and 40° with a step size of 0.017° and a counting time of 50 s per step. These measurements were performed to identify the type of solid species present in equilibrium and also to check for differing solid state forms (solvates and/or polymorphs).

2.7. Molecular Modeling. Molecular modeling studies were conducted to gain a deeper understanding of the solute−solvent interactions between the mandelic acid and the mandelate molecules. The calculations of the enthalpies of formation were performed on the basis of single-point energy calculations of solute−solvent dimers (where the dimer comprises the solute and solvent structures joined by hydrogen bonds) by employing the VAMP model in Materials Studio (Accelrys Materials Studio 4.3). The single-point energy calculation involves the computation of the wave function and charge density, and consequently the energy for a given molecule with a well-specified geometric structure.[29] The VAMP model uses semiempirical calculations that are based on this single-point energy calculation.

The enthalpy of formation (ΔH_{form}) was obtained by first performing a geometry and structure optimization of the single molecule setting the charge on each molecule to zero. Afterward, a dimer was created between the optimized solute and the solvent molecules, and the dimer with the more negative enthalpy of formation was selected as the optimized dimer. The geometry and structure optimization was conducted with the VAMP model together with Austin model 1 (AM1), and also the Neglect of Diatomic Differential Overlap (NDDO). The VAMP model was used together with AM1, which gives a good estimation for hydrogen bonding calculations. AM1 was designed to eliminate the problems from MNDO (modified neglect of differential overlap) caused by the tendency to overestimate repulsion between atoms separated by the sum of their van der Waals radii.[30] The NDDO is a basic approximation for neglecting less important integrals. When the VAMP model from the Materials Studio interface is used, then AM1 is the default NDDO Hamiltonian.[31]

From the obtained optimized structure, the heat of formation was essentially calculated using the same procedure explained above. The stability of a dimer was given by the heat of formation (ΔH_{form}^{dimer}), where the most stable dimer possesses the most negative value for ΔH_{form}^{dimer} and vice versa. More information with regard to the approach used is given in refs 32 and 33 and the Accelrys software manual.[34]

3. Results and Discussion

3.1. Characterization of the Chiral Task-Specific Solvents. To ensure a small selection of chiral task-specific solvents, a variety of mandelic acid esters were synthesized via an esterification reaction and subsequently used. The chemical and physical characteristics of the chiral solvents prepared are summarized in Table 2. As expected, the size and structure of the aliphatic rest of the ester were found to have a direct influence on the melting temperature. The same effect was also reported by Yalkowsky et al. for the physicochemical and crystalline properties of alkyl *p*-aminobenzoates.[35] The melting point indicates the lowest usable temperature of the chiral solvent. On the other hand, the high boiling temperatures facilitate applicability even at higher temperatures, although for crystallization-based investigations mostly lower temperatures are used (Mandelic acid decomposition occurs at elevated temperatures[36,37]). To quantify the asymmetric effects, two chiral task-specific solvents with a low melting point [(*S*)-*n*-propyl mandelate] and a higher melting point [(*S*)-*n*-isopropyl mandelate] were chosen for all further studies. These chiral solvents, chemically bonded on a cyclodextrin

Table 2. Chemical and Physical Properties of the Chiral Task-Specific Solvents

name	alkyl residue (−)	molecular formula (−)	molecular weight	melting point[b] (°C)	melting enthalpy (J/g)	boiling point (°C)	rotation angle (deg)
(*S*)-methyl mandelate	CH_3	$C_9H_{10}O_3$	166.2	55.0[c]	80.8	263.8	not determined
(*S*)-ethyl mandelate	C_2H_5	$C_{10}H_{12}O_3$	180.2	28.5	86.7	∼272[d]	−46.5
(*S*)-*n*-propyl mandelate[a]	*n*-C_3H_7	$C_{11}H_{14}O_3$	194.2	20.5	68.0	214.6	−60.9
(*S*)-isopropyl mandelate	*i*-C_3H_7	$C_{11}H_{14}O_3$	194.2	43.3	105.3	223.6	−60.8

[a] Viscosity of (*S*)-*n*-propyl mandelate: 99.2 mPa/s at 24 °C. [b] The onset temperature from the DSC experiment was used for the determination of the melting temperature. [c] Because of impurities within the commercially available (*S*)-methyl mandelate, the peak temperature was used for this solvent. [d] The high viscosity of this solvent decreases the accuracy of the measurement.

stationary phase, were also used successfully for the chromatographic resolution of mandelic acid derivatives.[38]

3.2. Differences in Solution Thermodynamics. The formation of diastereomeric adducts should cause direct changes of the thermodynamic parameters. Differences in the solubilities of the two enantiomers with the chiral solvent can be easily found. The more stable adducts will possess higher solubilities. Furthermore, the magnitude of the corresponding changes is a good indicator of the estimation of the stability of both diastereomeric adducts.

The results obtained from the solubility measurements of (*S*)-mandelic acid and (*R*)-mandelic acid in (*S*)-*n*-propyl mandelate are shown in Figure 3. It can be determined that the solubility of the (*R*)-mandelic acid is higher compared to that of the (*S*)-mandelic acid. This shows clearly that a pronounced asymmetric behavior is present with a difference in solubility of ∼2 wt %. These measurable differences in the solubilities of the (*S*)- and (*R*)-mandelic acid enantiomers indicate that there are enantioselective interactions of the chiral molecules with the chiral solvent and chiral recognition in the liquid phase.

A similar solubility difference for the enantiomers was found for the higher-melting solvent (*S*)-isopropyl mandelate at 50 °C (Table 3) with a solubility difference of ∼3.4 wt %. Again, in the chiral *S*-configurated solvents, (*R*)-mandelic acid was more soluble than the *S*-enantiomer. As in chiral solvents, the solubility of racemic mandelic acid significantly exceeded the solubility of the enantiomers.

The results for the chiral task-specific solvents (*S*)-isopropyl mandelate and (*S*)-*n*-propyl mandelate clearly show that a small, but significant, asymmetric effect is generated during the contact with the enantiomers of mandelic acid. On the basis of these results, the diastereomeric adduct between the solute (*R*)-mandelic acid and the (*S*)-mandelate seems to be more stable as the counterpart (*S*)-mandelic acid and (*S*)-mandelate.

To ensure the existence of the same mandelic acid solid phases during the solubility experiments, XRPD patterns were measured for the corresponding solid phases. Figure 4 shows selected results for (*S*)-isopropyl mandelate as the solvent. Reference patterns of the chiral species are included to compare the results. In all cases, the reflexes of the racemic compound and/or the mandelic acid enantiomer are clearly distinguishable; e.g., the reflex at 6.0° is typical for the enantiomer, and the reflexes at 10.8° and 33.2° are typical for the racemic compound. From the results of the crystal lattice analysis via XRPD, no additional or new phases were identified other than the racemic compound and the enantiomers. Thus, as expected, postulated adducts between the chiral solvent and the mandelic acid species are limited to the liquid phase.

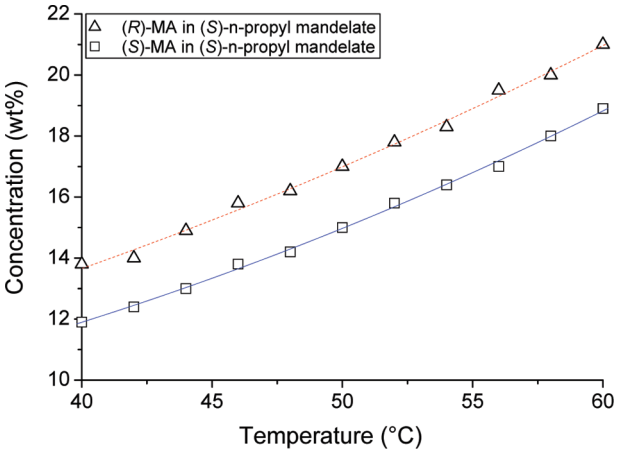

Figure 3. Solubility of (*S*)-mandelic acid and (*R*)-mandelic acid in (*S*)-*n*-propyl mandelate as a function of temperature (polythermal method). MA, mandelic acid.

3.3. Differences in Crystallization Kinetics. Enantioselective interactions between a chiral solute and a chiral solvent in solution should also influence crystallization kinetics, in particular nucleation rates. The respective characteristic values, the metastable zone widths, were found indeed to be different for both enantiomers. Figure 5 depicts the determined metastable zone width with respect to primary nucleation for (*R*)- and (*S*)-mandelic acid in (*S*)-*n*-propyl mandelate at 50 °C. It can clearly be seen that the MSZW increases with increasing cooling rate, which is consistent with the behavior in achiral solvents. The asymmetry effect continues with differences in the maximal possible undercooling. (*S*)-Mandelic acid is nucleated before (*R*)-mandelic acid. For racemic mandelic acid, it became evident that there exists a particular kinetic inhibition for crystallization from (*S*)-*n*-propyl mandelate. No nucleation was observed in the range of measurements (the lowest temperature being 20 °C).

The same type of inhibition effect was noticed in the case of the mandelic acid−(*S*)-ethyl lactate system, but in contrast here, only one of the enantiomers did not nucleate while the racemic mandelic acid did crystallize first.[21]

In the presence of a chiral selective additive, the well-known "rule of reversal" is applied.[26,39−41] It means the additive is stereoselectively adsorbed at the surface of growing

Table 3. Mandelic Acid Solubilities in (*S*)-Isopropyl Mandelate at 50 °C (isothermal method, average of two experiments)

solvent	(*S*)-mandelic acid (wt %)	(*R*)-mandelic acid (wt %)	racemic mandelic acid (wt %)
(*S*)-isopropyl mandelate	18.4	21.8	36.0

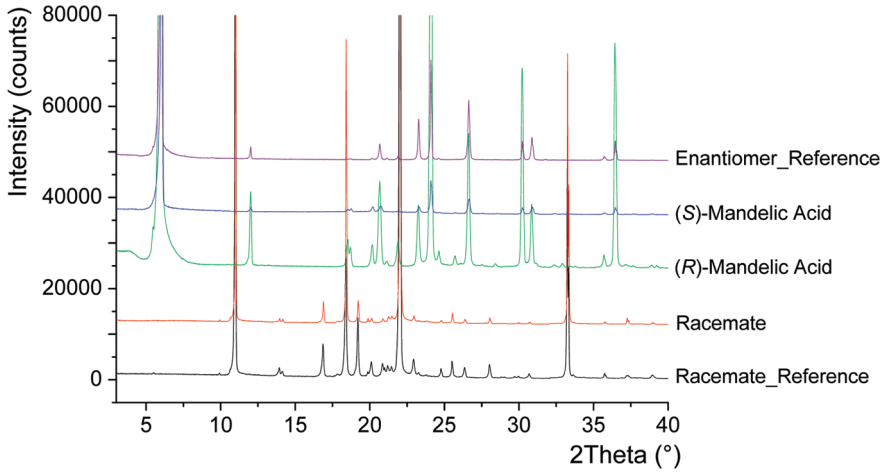

Figure 4. XRPD patterns for pure enantiomers and the racemate of mandelic acid, and from solubility experiments in (*S*)-isopropyl mandelate at 50 °C.

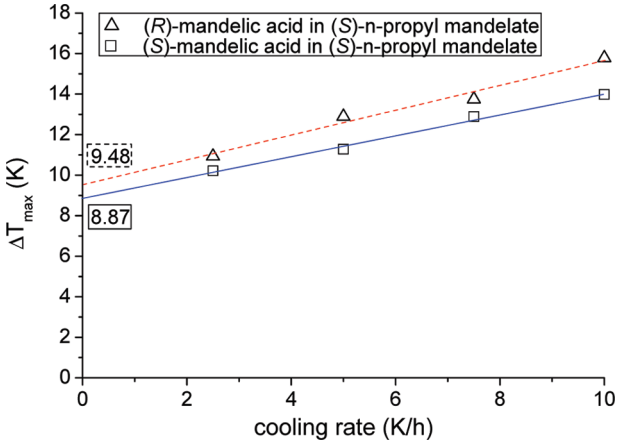

Figure 5. Metastable zone width with respect to primary nucleation for the mandelic acid species in (*S*)-*n*-propyl mandelate at 50 °C (T_{sat}). The boxed numbers represent the extrapolated results for a hypothetical cooling rate of 0 K/h.

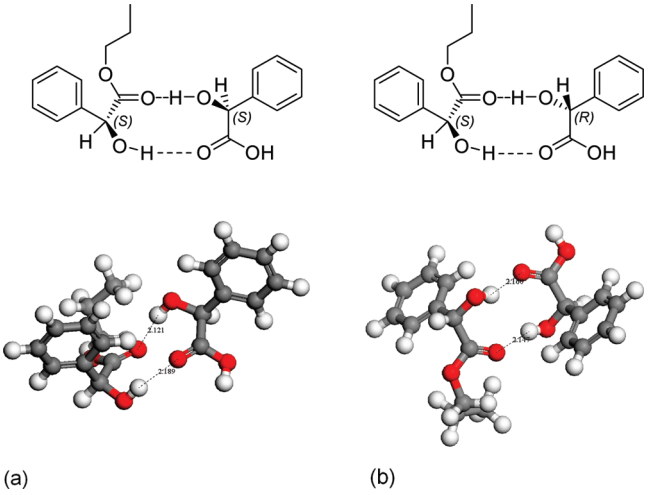

Figure 6. Schematic representation of the optimized molecular structures of (a) (*S*)-mandelic acid and (*S*)-*n*-propyl mandelate and (b) (*R*)-mandelic acid and (*S*)-*n*-propyl mandelate, connected via hydrogen bonds.

crystals of the enantiomer of the same absolute configuration, resulting in a strong reduction in their growth rate and hence allowing for preferential crystallization of the opposite enantiomer. In our studies, obviously the rule of reversal is not obeyed because the *S*-configured chiral solvent inhibits nucleation of the *R*-enantiomer of mandelic acid. This unusual effect was also reported recently by Medina et al. for the enantioselective crystallization in the presence of chiral polymeric microspheres.[42] However, the obtained nucleation behavior correlates with the presence of more stable (*R*)-mandelic acid−(*S*)-*n*-propyl mandelate adducts in the solution phase. Because of the strong solvent−(*R*)-mandelic acid interactions, nucleation of (*R*)-mandelic acid is inhibited compared to (*S*)-mandelic acid being less strongly solvated.

3.4. Molecular Modeling of Interactions between Mandelic Acid and the Propyl Mandelates. We determined whether the origin of the observed asymmetric behavior obtained can be explained or better understood on a molecular level. Therefore, diastereomeric adducts of the solute mandelic acid and the chiral solvents were postulated (Figure 6). Hydrogen bonds were formed between the carbonyl function of the mandelate and the hydroxyl group of the mandelic acid enantiomer and between the hydroxyl group of the mandelate and the carbonyl function of the mandelic acid enantiomer. This behavior was adopted from the crystal structure of mandelic acid and related (racemic) mandelates, which showed a similar behavior.[43−46] The stabilization enthalpies ($\Delta H_{form}^{stabilization}$) were derived from the enthalpy of formation of the dimer molecules (ΔH_{form}^{dimer}) minus the enthalpy of formation of the single molecules of the solute (ΔH_{form}^{solute}) and the solvent ($\Delta H_{form}^{solvent}$). Davey et al. reported that mandelic acid in all solvents except chloroform in solution is strongly solvated.[5] Therefore, the $\Delta H_{form}^{stabilization}$ values were derived by subtraction of the summation of the single molecules ($\Delta H_{form}^{solute} + \Delta H_{form}^{solvent}$) from that of the dimer (ΔH_{form}^{dimer}). Noteworthy is the fact that other hydrogen bond-forming solvents (water, alcohol, etc.) need to be removed strictly from the enantiopure solvents to prevent the destruction of the diastereomeric solvent−solute adducts, causing a weakening or even a loss of the asymmetric effect.

The molecular modeling results are summarized in Table 4. They support the determined solubility and MSZW values given above. The diastereomeric adducts of (*R*)-mandelic acid with (*S*)-*n*-propyl mandelate and (*R*)-mandelic acid with (*S*)-isopropyl mandelate are characterized by $\Delta H_{form}^{stabilization}$

Table 4. Summary of ΔH_{form} Values of Individual Molecules and Dimers of (*S*)- or (*R*)-Mandelic Acid (MA) with (*S*)-*n*-Propyl Mandelate [(*S*)-PM] or (*S*)-Isopropyl Mandelate [(*S*)-IPM]

single-molecule energy		dimer energy		
single molecule	$\Delta H_{form}^{solute/solvent}$ (kcal/mol)	dimer type	ΔH_{form}^{dimer} (kcal/mol)	$\Delta H_{form}^{stabilization}$ [$\Delta H_{form}^{dimer} - (\Delta H_{form}^{solute} + \Delta H_{form}^{solvent})$] (kcal/mol)
(*S*)-MA	−117.56			
(*S*)-PM	−122.97	(*S*)-MA−(*S*)-PM	−243.31	−2.78
(*R*)-MA	−117.56			
(*S*)-PM	−122.97	(*R*)-MA−(*S*)-PM	−246.00	−5.47
(*S*)-MA	−117.56			
(*S*)-IPM	−120.99	(*S*)-MA−(*S*)-IPM	−242.52	−3.97
(*R*)-MA	−117.56			
(*S*)-IPM	−120.99	(*R*)-MA−(*S*)-IPM	−244.42	−5.87

values of −5.47 and −5.87 kcal/mol, respectively, slightly more negative than for the counter enantiomer, (*S*)-mandelic acid in (*S*)-*n*-propyl mandelate and (*S*)-isopropyl mandelate (−2.78 and −3.97 kcal/mol, respectively). More negative heats of formation result in a more thermodynamically stable dimer connected with higher solubilities and a lower probability of nucleation for the corresponding mandelic acid enantiomer. The more strongly solvated, the more energy is required for desolvation as the first step for formation of mandelic acid nuclei.

Moreover, the comparison of the mandelic acid solubilities in (*S*)-isopropyl and (*S*)-*n*-propyl mandelate is in agreement with the molecular modeling results. The stabilization enthalpies are more negative for the isopropyl mandelate−mandelic acid dimers than for the *n*-propyl mandelate−mandelic acid dimers, proof of the higher solubilities of mandelic acid in isopropyl mandelate.

4. Conclusion

In this work, chiral task-specific solvents and their interdependencies with the chiral solutes were investigated and discussed. Different mandelic acid esters were used as chiral task-specific solvents. They have an asymmetric effect on the thermodynamic and kinetic properties of the enantiomers of mandelic acid. The results show the general effect of dissimilarity, but only moderate changes were found. Further, via molecular modeling, the origin of these effects was postulated as the formation of a diastereomeric adduct in solution, formed by one solvent and one solute molecule, which are connected via hydrogen bonds. In agreement with the experimental results, a more stable adduct of (*S*)-mandelate and (*R*)-mandelic acid compared to (*S*)-mandelate and (*S*)-mandelic acid was found.

With regard to a resolution process, the yield of the less soluble (*S*)-mandelic acid might be increased by exploitation of the wide MSZW of the more soluble (*R*)-mandelic acid. It should be possible to crystallize (*S*)-mandelic acid under conditions where (*R*)-mandelic acid is already supersaturated but still in the metastable zone. Planned further studies will be devoted to determining the whole asymmetric ternary (solubility) phase diagram and should together with additional kinetic investigations clarify the observed effects in more detail.

Acknowledgment. We thank Jacqueline Kaufmann, Luise Borchert, Chandrakant Malwade, and Nora Doering for their help in the experimental work. NMR spectra were recorded at the Otto von Guericke University in Magdeburg by Dr. Liane Hilfert. This work was partially funded by the European Union [EU-project "IntEnant, Integrated Synthesis and Purification of Enantiomers" (NMP2-SL-2008-214129)].

References

(1) Caner, H.; Groner, E.; Levy, L.; Agranat, I. *Drug Discovery Today* **2004**, *9*, 105–110.
(2) Collins, A. N.; Sheldrake, G. N.; Crosby, J. *Chirality in Industry: The Commercial Manufacture and Applications of Optically Active Compounds*; Wiley & Sons: Chichester, U.K., 1992.
(3) Jacques, J.; Collet, A.; Wilen, S. H. *Enantiomers, Racemates and Resolutions*; Krieger Publishing Co.: Malabar, FL, 1994.
(4) Mullin, J. W. *Crystallization*; Butterworth-Heinemann: Oxford, U.K., 1997; p 600.
(5) Davey, R. J. In *Solvent effects in crystallisation processes*; Kaldis, E., Ed.; North-Holland Publishing Co.: Amsterdam, 1982; Vol. 8, pp 429−479.
(6) Wang, X. J.; Yang, X.; Liu, Y. X.; Ching, C. B. *AIChE J.* **2008**, *54*, 2281–2292.
(7) Fidler, J.; Rodger, P. M.; Rodger, A. *J. Am. Chem. Soc.* **1994**, *116*, 7266–7273.
(8) Mizuno, Y.; Aida, T.; Yamaguchi, K. *J. Am. Chem. Soc.* **2000**, *122*, 5278–5285.
(9) Khatri, C. A.; Pavlova, Y.; Green, M. M.; Morawetz, H. *J. Am. Chem. Soc.* **1997**, *119*, 6991–6995.
(10) Ishi-i, T.; Crego-Calama, M.; Timmerman, P.; Reinhoudt, D. N.; Shinkai, S. *J. Am. Chem. Soc.* **2002**, *124*, 14631–14641.
(11) Reichardt, C. *Solvents and Solvent Effects in Organic Chemistry*; Wiley VCH: Weinheim, Germany, 2003; p 653.
(12) Celebre, G.; De Luca, G.; Maiorino, M.; Iemma, F.; Ferrarini, A.; Pieraccini, S.; Spada, G. P. *J. Am. Chem. Soc.* **2005**, *127*, 11736–11744.
(13) Leeman, M.; Brasile, G.; Gelens, E.; Vries, T.; Kaptein, B.; Kellogg, R. *Angew. Chem., Int. Ed.* **2008**, *47*, 1287–1290.
(14) Yu, J.; RajanBabu, T. V.; Parquette, J. R. *J. Am. Chem. Soc.* **2008**, *130*, 7845–7847.
(15) Solntsev, K. M.; Tolbert, L. M.; Cohen, B.; Huppert, D.; Hayashi, Y.; Feldman, Y. *J. Am. Chem. Soc.* **2002**, *124*, 9046–9047.
(16) Yamamoto, M.; Yamamoto, Y. *Inorg. Nucl. Chem. Lett.* **1975**, *11*, 833–836.
(17) Amaya, K. *Bull. Chem. Soc. Jpn.* **1961**, *34*, 1803–1806.
(18) Bosnich, B.; Watts, D. W. *J. Am. Chem. Soc.* **1968**, *90*, 6228–6230.
(19) Mizumachi, K. *J. Coord. Chem.* **1973**, *3*, 191–192.
(20) Tulashie, S. K.; Lorenz, H.; Hilfert, L.; Edelmann, F. T.; Seidel-Morgenstern, A. *Cryst. Growth Des.* **2008**, *8*, 3408–3414.
(21) Tulashie, S. K.; Lorenz, H.; Seidel-Morgenstern, A. *Cryst. Growth Des.* **2009**, *9*, 2387–2392.
(22) Lüttringhaus, A.; Berrer, D. *Tetrahedron Lett.* **1959**, 10–12.
(23) Buhse, T.; Kondepudi, D. K.; Hoskins, B. *Chirality* **1999**, *11*, 343–348.
(24) Doki, N.; Yokota, M.; Sasaki, S.; Kubota, N. *Cryst. Growth Des.* **2004**, *4*, 1359–1363.
(25) Lahav, M.; Leiserowitz, L. *J. Phys. D: Appl. Phys.* **1993**, *26*, B22–B31.
(26) Addadi, L.; Vanmil, J.; Lahav, M. *J. Am. Chem. Soc.* **1981**, *103*, 1249–1251.
(27) Basavaiah, D.; Krishna, P. R. *Tetrahedron* **1995**, *51*, 2403–2416.
(28) Nyvlt, J. *Collect. Czech. Chem. Commun.* **1980**, *45*, 1920–1927.
(29) Pople, J. A. *Approximate Molecular Orbital Theory*; McGraw-Hill: New York, 1970; p 224.
(30) Dewar, M. J. S.; Zoebisch, E. G.; Healy, E. F.; Stewart, J. J. P. *J. Am. Chem. Soc.* **1985**, *107*, 3902–3909.
(31) Pople, J. A.; Segal, G. A. *J. Chem. Phys.* **1965**, *44*, 3289–3296.
(32) Hinchliffe, A. *Molecular Modelling for Beginners*; John Wiley & Sons Ltd.: Chichester, U.K., 2008; p 428.

(33) Frenkel, D.; Smit, B. *Understanding Molecular Simulation: From Algorithms to Applications* (*Computational Science*); Academic Press: San Diego, 2001.
(34) *Materials Studio Release Notes*, release 4.3; Accrelys Software Inc.: San Diego, 2008.
(35) Yalkowsky, S. H.; Slunick, T. G.; Flynn, G. L. *J. Pharm. Sci.* **1972**, *61*, 852–857.
(36) Hurd, C. D.; Raterink, H. R. *J. Am. Chem. Soc.* **1933**, *55*, 1541–1546.
(37) Domingo, L. R.; Picher, M. T.; Andres, J.; Safont, V. S.; Chuchani, G. *Chem. Phys. Lett.* **1997**, *274*, 422–428.
(38) Fujimura, K.; Kitagawa, M.; Takayanagi, H.; Ando, T. *J. Liq. Chromatogr.* **1986**, *9*, 607–620.
(39) Zbaida, D.; Lahav, M.; Drauz, K.; Knaup, G.; Kottenhahn, M. *Tetrahedron* **2000**, *56*, 6645–6649.
(40) Addadi, L.; Weinstein, S.; Gati, E.; Weissbuch, I.; Lahav, M. *J. Am. Chem. Soc.* **1982**, *104*, 4610–4617.
(41) Ndzie, E.; Cardinael, P.; Petit, M. N.; Coquerel, G. *Enantiomer* **1999**, *4*, 97–101.
(42) Medina, D. D.; Goldshtein, J.; Margel, S.; Mastai, Y. *Adv. Funct. Mater.* **2007**, *17*, 944–950.
(43) Davey, R. J.; Dent, G.; Mughal, R. K.; Parveen, S. *Cryst. Growth Des.* **2006**, *6*, 1788–1796.
(44) Mughal, R. K.; Pritchard, R. G.; Davey, R. J. *Acta Crystallogr.* **2004**, *E60*, O1984–O1986.
(45) Fischer, A.; Profir, V. M. *Acta Crystallogr.* **2003**, *E59*, O1113–O1116.
(46) Patil, A. O.; Pennington, W. T.; Paul, I. C.; Curtin, D. Y.; Dykstra, C. E. *J. Am. Chem. Soc.* **1987**, *109*, 1529–1535.